THE JOURNAL OF BIOLOGICAL CHEMISTRY
Vol. 277, No. 30, Issue of July 26, pp. 27353–27359, 2002
Printed in U.S.A.
© 2002 by The American Society for Biochemistry and Molecular Biology, Inc.

Hsc66 Substrate Specificity Is Directed toward a Discrete Region of the Iron-Sulfur Cluster Template Protein IscU*

Received for publication, March 22, 2002, and in revised form, May 2, 2002
Published, JBC Papers in Press, May 6, 2002, DOI 10.1074/jbc.M202814200

Kevin G. Hoff, Dennis T. Ta, Tim L. Tapley, Jonathan J. Silberg‡, and Larry E. Vickery§

From the Department of Physiology and Biophysics, University of California, Irvine, California 92697

Hsc66 and Hsc20 comprise a specialized chaperone system important for the assembly of iron-sulfur clusters in *Escherchia coli*. Only a single substrate, the Fe/S template protein IscU, has been identified for the Hsc66/Hsc20 system, but the mechanism by which Hsc66 selectively binds IscU is unknown. We have investigated Hsc66 substrate specificity using phage display and a peptide array of IscU. Screening of a heptameric peptide phage display library revealed that Hsc66 prefers peptides with a centrally located Pro-Pro motif. Using a cellulose-bound peptide array of IscU we determined that Hsc66 interacts specifically with a region (residues 99–103, LPPVK) that is invariant among all IscU family members. A synthetic peptide (ELPPVKIHC) corresponding to IscU residues 98–106 behaves in a similar manner to native IscU, stimulating the ATPase activity of Hsc66 with similar affinity as IscU, preventing Hsc66 suppression of bovine rhodanese aggregation, and interacting with the peptide-binding domain of Hsc66. Unlike native IscU, however, the synthetic peptide is not bound by Hsc20 and does not synergistically stimulate Hsc66 ATPase activity with Hsc20. Our results indicate that Hsc66 and Hsc20 recognize distinct regions of IscU and further suggest that Hsc66 will not bind LPPVK motifs with high affinity *in vivo* unless they are in the context of native IscU and can be directed to Hsc66 by Hsc20.

Hsc66 (HscA) is a 66-kDa heat shock cognate protein in *Escherichia coli* that belongs to the Hsp70 class of molecular chaperones (1, 2). As found for Hsp70 family members, Hsc66 displays slow intrinsic ATPase activity (2–4), the ability to suppress the aggregation of denatured model peptides (3), and nucleotide dependent binding of substrate proteins (3, 5). Hsc66 is regulated by a J-type co-chaperone, Hsc20 (HscB), which stimulates Hsc66 ATPase activity (2) and enhances Hsc66 substrate binding (6). In contrast to other Hsp70s, however, only a single protein substrate, IscU, has been identified for Hsc66 (5). IscU is a highly conserved 14-kDa protein that can form reduction-labile 2Fe-2S and 4Fe-4S clusters (6–9). The ability of IscU to form clusters *in vitro* suggests that it may function as a scaffold for the assembly of iron-sulfur clusters (6, 9), and Hsc66 and Hsc20 may comprise a specialized chaperone system that participates in the biogenesis of iron-sulfur proteins. Mutational analysis of the genes encoding Hsc66, Hsc20, and IscU support this idea (10). In addition, homologs of these proteins with similar functions have also been identified in higher organisms suggesting that this specialized system has been conserved throughout evolution (11–15).

The structural determinants required for Hsc66 binding to substrates remain unknown. Furthermore, it is unclear whether the physiological function of Hsc66 involves recognition of a specific peptide motif or whether Hsc66 interacts with a wide array of peptide substrates. DnaK, the other major Hsp70 present in *E. coli*, exhibits broad substrate specificity (16, 17). Phage display, peptide array, and structural studies reveal that DnaK prefers unfolded peptides approximately eight amino acids in length and enriched by hydrophobic residues flanked at either end by basic residues (16–18). This general type of motif is found in most proteins and occurs on average every 36 amino acids; because of this DnaK interacts with a large percentage of cellular proteins, and many proteins have multiple DnaK-binding sites (17). Hsc66 shares 42% sequence identity with DnaK but differs at residues found to be important for DnaK binding to substrates (3, 18). This may impart Hsc66 with different substrate specificity than DnaK, and several lines of evidence support this possibility. *In vivo* studies have shown that Hsc66 is incapable of substituting for DnaK, because a *dnaK*− strain of *E. coli* is inviable at high temperatures (19), and Hsc66 is not able to prevent bulk protein aggregation in these cells (20). *In vitro*, Hsc66 is capable of preventing the aggregation of denatured model substrates, but it does this with differing specificity than DnaK (3). Finally, Hsc66 has been found to interact with native IscU, whereas IscU stimulates DnaK ATPase only weakly (6).

To gain understanding of the structural determinants of substrates important for Hsc66 binding we have used two different approaches. First, we examined Hsc66 binding to an unconstrained library of peptide heptamers displayed in a phage library. Second, to determine whether there is a correlation between peptides selected in the phage library and Hsc66 recognition of IscU, as well as to determine whether Hsc66 binds IscU in a specific location or at various sites, we screened a cellulose array displaying the entire sequence of IscU as overlapping peptides 13 amino acids in length. Peptides identified by both approaches have been synthesized and their effects on Hsc66 ATPase activity have been examined. We have found that Hsc66 prefers peptides with centrally located proline residues and, consistent with this finding, Hsc66 binds specifically to one region of IscU that displays the sequence LPPVK.

* This work was supported by National Institutes of Health Grant GM54264, National Institutes of Health Training Grant GM07211 (to K. G. H.), and National Institutes of Health (NCI) Carcinogenesis Training Program Grant 5T32CA09054 (to T. L. T.). The costs of publication of this article were defrayed in part by the payment of page charges. This article must therefore be hereby marked "*advertisement*" in accordance with 18 U.S.C. Section 1734 solely to indicate this fact.

‡ Current address: Dept. of Chemical Engineering, California Institute of Technology, Pasadena, CA 91125.

§ To whom correspondence should be addressed: Dept. of Physiology and Biophysics, University of California, Irvine, CA 92697. Tel.: 949-824-6580; Fax: 949-824-8540; E-mail: lvickery@uci.edu.

This is an Open Access article under the CC BY license.

EXPERIMENTAL PROCEDURES

Materials—E. coli DH5αFIQ cells were from Invitrogen and BL–21(DE3)pLysS cells were from Novagen. Materials for Fmoc[1] peptide synthesis were from NovaBiochem. Bacterial growth media components were from Difco, and other reagents were from Sigma.

Overexpression and Purification of Proteins—Recombinant Hsc66, Hsc66:2-382, Hsc66:2-505, Hsc20, DnaK, and IscU were expressed and purified as previously described (2, 3, 5, 6).

Phage Display Peptide Panning—Phage display experiments were conducted using the PH.D-7 phage library (New England Biolabs) as directed by the manufacturer with slight modifications as follows. Briefly, M13 phage with a random seven-residue peptide encoded at the N terminus of the pIII protein were incubated with immobilized Hsc66 in HKM buffer (50 mM Hepes, pH 7.3, 150 mM KCl, and 10 mM $MgCl_2$) supplemented with 1 mM ADP. Unbound phage were washed (three times, 20 min each), and bound phage were released using HKM buffer supplemented with 1 mM ATP. Bound phage were amplified, and after three rounds of enrichment 133 phage were selected, their DNA sequenced, and the heptameric peptide sequence was deduced from translation of the nucleotide sequence. Data for the 70 phage from the naïve library were provided by the manufacturer.

Electroblot Analysis of Cellulose-bound IscU Peptides—The cellulose-bound peptide scan of the entire IscU sequence consisted of 53 13–residue peptides overlapping by 11 amino acids and anchored via a C-terminal Ala_2 linkage (Jerini Bio Tools GmbH, Berlin, Germany). For analysis of chaperone binding, either Hsc66 or DnaK (5 μM) were incubated with the membrane in HKM buffer supplemented with 1 mM ADP at room temperature for 1 h. The membrane was washed two times (10 min each) at room temperature with HKM containing 1 mM ADP. Bound protein was transferred to polyvinylene difluoride membranes via electroblotting with a semi-dry blotter using a constant current of 0.8 mA/cm^2. Protein transferred to polyvinylene difluoride was visualized by affinity-purified polyclonal rabbit antisera to Hsc66 (or anti-DnaK mouse monoclonal antibody; Stressgen) using enhanced chemiluminescence detection (Amersham Biosciences). For studies of Hsc20 effects, 50 μM Hsc20 was added to Hsc66 in HKM buffer with 1 mM ADP prior to incubation of the blot. Hsc20 binding to the array was carried out in HKM buffer using 50 μM Hsc20 in the absence of Hsc66.

Peptide Synthesis—IscU peptide E98-C106 and phage display peptide PD1 were prepared by the Stanford core facility (Palo Alto, CA) or synthesized using standard Fmoc chemistry (21). Peptides were subsequently purified by reverse phase high pressure liquid chromatography and their composition was confirmed by matrix-assisted laser desorption ionization time-of-flight mass spectrometry. Peptide concentrations were determined by Ellman's reagent (22) upon reaction with the C-terminal cysteine of IscU E98-C106 or UV absorbance based on an extinction coefficient of 5,600 $(M\ cm)^{-1}$ at 280 nm for PD1 based on a single tryptophan residue (23–25).

ATPase Assays—Steady-state ATPase rates were determined at 23 °C in HKM buffer containing 1 mM dithiothreitol and 1.5 mM ATP by measuring phosphate released using the EnzCheck-coupled enzyme phosphate assay kit (Molecular Probes) as previously reported (2, 3, 5, 6). Under these conditions Hsc66 has a basal turnover number of 0.12 min^{-1}. Error bars for all figures are shown when they fall outside the symbol used.

Rhodanese Aggregation Assays—The aggregation of bovine rhodanese was performed in HKM buffer containing 1 mM ADP as described previously (3, 5). Hsc66 was incubated with peptide or IscU for 10 min at 25 °C prior to addition of denatured rhodanese and changes in turbidity were monitored in a Cary 1 spectrophotometer (Varian Inc.) at 320 nm.

RESULTS

Hsc66 Binding to Phage-displayed Peptides—Phage display libraries have been used to establish peptide binding specificities for the *E. coli* Hsp70 DnaK (16), bovine Hsc70 (26), and the eukaryotic endoplasmic reticulum chaperone BiP (27), and each of these hsp70s were found to prefer peptides with a high content of centrally located hydrophobic residues. To determine whether Hsc66 binds preferentially to peptides of similar sequences we screened a M13 coliphage peptide display library for Hsc66 binding. The coliphage in these experiments carry a random 7-amino acid extension linked by a –Gly_3–Ser– sequence at the N terminus of the pIII surface protein.

Sequences	# Selected	% selected
S L W **P** **P** V S	44	33.1
M S **P** I L S **P**	26	19.5
I T Q **P** S L R	8	6.0
F K S L **P** M **P**	8	6.0
G R **P** L **P** **P** S	5	3.8
Q S T Q S **P** L	5	3.8
A H N S A A D	5	3.8
A E G **P** **P** N E	4	3.0
F G S H A S E	3	2.3
S A A L **P** A R	3	2.3
N W L **P** T **P** **P**	2	1.5
L V S T **P** L **P**	2	1.5
K V **P** W I S W	2	1.5
S A R L **P** A R	2	1.5
V A K I W V D	2	1.5
T S T T H T R	2	1.5
G L S **P** A T S	2	1.5
M S K **P** T **P** L	1	0.75
I Q **P** F T L Q	1	0.75
S A G L **P** A R	1	0.75
I V Y R T S S	1	0.75
T Y Q R A L Y	1	0.75
N R T M A **P** W	1	0.75
R S M Q M **P** **P**	1	0.75
T M S L **P** H H	1	0.75

FIG. 1. **Amino acid sequences of heptapeptides displayed by coliphage selected for binding to Hsc66.** DNA was purified from 133 M13 clones selected after three rounds of binding to Hsc66·ADP and elution via ATP. The sequences of the heptapeptides displayed by these phage were deduced from the nucleotide sequence of the corresponding region of the pIII gene of the coliphage. Proline residues are shown in *bold* (**P**).

Affinity panning experiments for Hsc66 binding were conducted using polystyrene plates that had been coated with Hsc66 and then blocked with bovine serum albumin. Phage were incubated with plates in the presence of 1 mM ADP to ensure that Hsc66 was in the high affinity R-state for substrate binding (4, 5). After washing, ADP-containing buffer was exchanged for buffer supplemented with 1 mM ATP, thereby converting Hsc66 to the low substrate affinity T-state and eluting specifically bound phage. After three rounds of enrichment, 133 phage were sequenced, and the amino acid sequences of the heptamers were determined. As shown in Fig. 1 25 unique heptameric sequences were identified. Two heptamers, SLWPPVS and MSPILSP, accounted for greater than 50% of the total identified phage. This differs from similar studies where a broad array of unique peptides was isolated for DnaK (16) and BiP (27).

The relative occurrence of the 20 amino acids in the selected phage was calculated by quantifying the number of times each amino acid occurred in the 133 heptamers and dividing by the total number of amino acids. These values were compared with the relative occurrence of each amino acid from 70 phage in the naïve library (Fig. 2*A*). Seven amino acids show increased occurrence among the bound phage. As seen for other chaperones (16, 17, 27, 28), hydrophobic residues (Ile, Val, and Leu) are over-represented. In addition, tryptophan, an amino acid favored by BiP, is enriched among Hsc66-bound phage, although this results largely from its presence in the most abundant peptide sequence, SLWPPVS. Of the 3 remaining amino acids that show enrichment in Hsc66-bound phage (Ser, Met, and Pro), methionine shows neutral contributions to the binding of substrates to BiP and DnaK. Serine is also a neutral contributor to DnaK, but is slightly selected against in BiP substrates. Proline shows neutral contributions to substrate binding to BiP, but is selected against in DnaK substrates (16, 17, 27). Cysteine is under-represented in the naïve library and was not analyzed.

[1] The abbreviations used are: Fmoc, *N*-(9-fluorenyl)methoxycarbonyl; E98-C106, synthetic peptide corresponding to residues 98–106 of *E. coli* IscU; PD1, synthetic peptide, SLWPPVS, corresponding to the most highly represented phage from affinity panning.

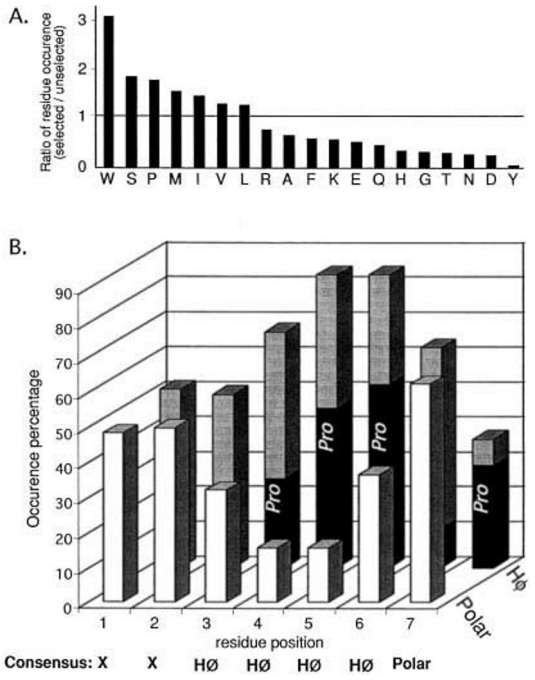

FIG. 2. **Relative abundance of amino acids in heptapeptides of phage selected by affinity panning.** *A*, the ratio of occurrence of each amino acid displayed in the heptapeptides of the 133 selected phage to the occurrence of the same amino acid in 70 phage selected randomly from the naïve library. Cysteine is under-represented in the naïve library and was not analyzed. *B*, occurrence percentage by position for a given amino acid type. Amino acids were classified as either polar (Arg, Lys, Asp, Glu, Ser, Gln, Asn, Thr, and His) or hydrophobic (Met, Ile, Leu, Val, Ala, Gly, Phe, Tyr, Trp, and Pro). The occurrence of proline is designated by *black shading* of the hydrophobic *bars*. A given amino acid class is designated in the consensus sequence if its occurrence percentage is at least 25% greater than the other amino acid class at a given position. The designation of *X* at positions 1 and 2 corresponds to an equal likelihood of either polar or hydrophobic residues.

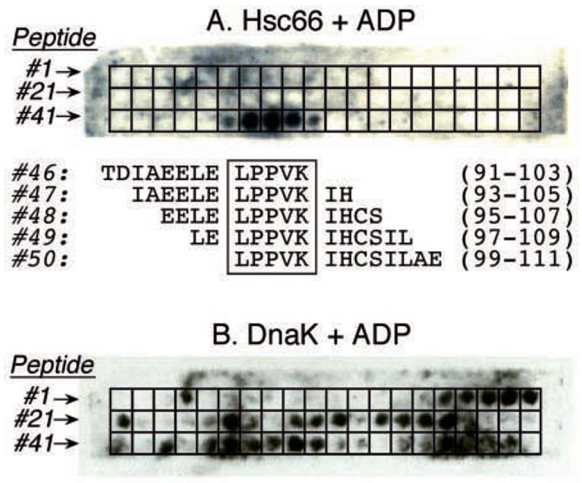

FIG. 3. **Chaperone binding to an IscU peptide array.** A nitrocellulose array of 13-mer peptides corresponding to the entire IscU primary sequence was incubated with 5 μM Hsc66 (*A*) or 5 μM DnaK (*B*) in HKM buffer containing 1 mM ADP. After washes, bound chaperone was electrotransferred to a polyvinylene difluoride membrane and proteins were visualized by immunoblotting and chemiluminescence. Sequences of peptides bound by Hsc66 are aligned, and common residues are *boxed*.

In addition to an enrichment of proline, 42% of the selected phage (56 of 133) contained two adjacent proline residues. This is a 10-fold increase over the naïve library in which only 4.3% (3 of 70) of the sequenced phage contained this motif. The strong preference for adjacent prolines arises in part because of the heptapeptide SLWPPVS found in 44 of 133 of the selected phage. However, the Pro-Pro motif is also present in 20% (5 of 25) of the unique phage peptide sequences selected by Hsc66; this remains a 5-fold increase over the naïve library. Adjacent proline residues were not identified as substrates for either DnaK or BiP in previous phage display studies (16, 27).

All other amino acids are disfavored for Hsc66 binding. As found for DnaK substrate specificity, acidic amino acids are under-represented in Hsc66-bound phage. However, aromatic residues tyrosine and phenylalanine and basic residues arginine and lysine that act as positive contributors to DnaK substrate binding are disfavored by Hsc66. Thus, not only does Hsc66 prefer residues disfavored by DnaK (proline), but it also disfavors positive contributors to DnaK substrate binding.

Analysis of the different classes of amino acids as a function of their position in the heptapeptide is shown in Fig. 2*B*. The profile displays a higher proportion of polar residues at the termini, whereas the central positions are dominated by hydrophobic amino acids. Positions one and two show no preference for either hydrophobic or polar amino acids with each class occupying these positions in about half of the phage. Hydrophobic residues predominate positions 3–6, with Pro accounting for greater than 50% of the hydrophobic amino acids at positions 4 and 5. Polar residues appear to be preferred at position 7. Based on this analysis, the consensus sequence for Hsc66-bound phage exhibits the pattern *X*-*X*-Hϕ-Pro-Pro-Hϕ-polar, where Hϕ is a hydrophobic residue (commonly Leu or Val) and *X* represents an equal likelihood of polar or hydrophobic residues. Because of the possibility that the high proportion of selected phage carrying either the SLWPPVS or MSPILSP heptapeptides may bias the consensus sequence, the data was also analyzed excluding either one of the peptides. The overall conclusions remained the same, and in both cases, the consensus sequence retained the Hϕ–Pro–Pro–Hϕ–polar motif.

Identification of Hsc66-binding Sites within IscU—To date, the Fe/S-escort protein IscU is the only natural substrate that has been identified for Hsc66 (5). To determine locations of Hsc66 binding in the IscU primary sequence, we utilized a cellulose-bound peptide array corresponding to the IscU sequence. The array contained peptides of 13 residues, a length shown to allow DnaK binding to similar blots of σ^{32} (29) and other proteins (17). Starting with the N terminus of IscU, successive peptides were shifted by 2 amino acids along the IscU sequence resulting in an overlap of 11 residues. Hsc66 was incubated with the array in HKM buffer containing 1 mM ADP to stabilize Hsc66 in the high affinity R-state for substrate binding (3–5). Incubation was carried out for 1 h, a time period ~10-fold longer than found necessary for Hsc66·ADP to reach equilibrium with native IscU in surface plasmon resonance experiments (5). The array was then washed to remove unbound Hsc66, and bound Hsc66 was electrotransferred to polyvinylene difluoride membranes and detected by immunoblot analysis. As shown in Fig. 3*A*, screening by this method revealed a single Hsc66-binding region that spans residues 91–111 of IscU. The five peptides identified share an overlapping 5-amino acid sequence, LPPVK (residues 99–103). The LPPVK sequence is in good agreement with the last 5 amino acids of the consensus sequence that was identified by phage display, Hϕ-Pro-Pro-Hϕ-polar (Fig. 2*B*).

To determine whether Hsc66 binding is specific for this region of IscU or is a function of general chaperone binding to the IscU blot, we conducted a similar experiment using DnaK. DnaK bound to five separate regions of the arrayed IscU sequence corresponding to 25 individual peptides (Fig. 3*B*). This number of binding sites is consistent with DnaK binding to other cellulose-peptide arrays in which DnaK-binding sites

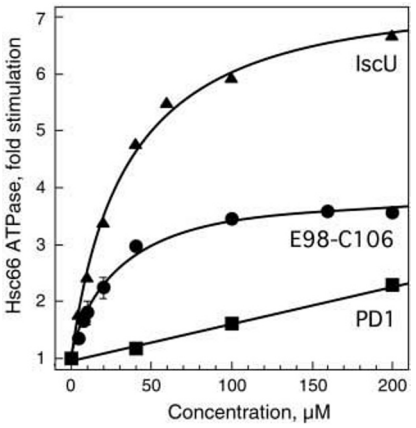

FIG. 4. **Effects of peptides on the ATPase activity of Hsc66.** Results are reported as the increase in the basal ATPase rate of Hsc66 in HKM buffer with 1.5 mM ATP at 23 °C. The *curves* shown represent best fits to the data for maximal stimulation of 7.7-fold and half-maximal stimulation at 33.7 μM for IscU (▲) and 4.02-fold and 26.6 μM for the IscU E98-C106 peptide (●). Maximal stimulation and affinity for PD1 (■) was not determined. *Error bars* for two experiments are shown where they fall outside of the symbols used.

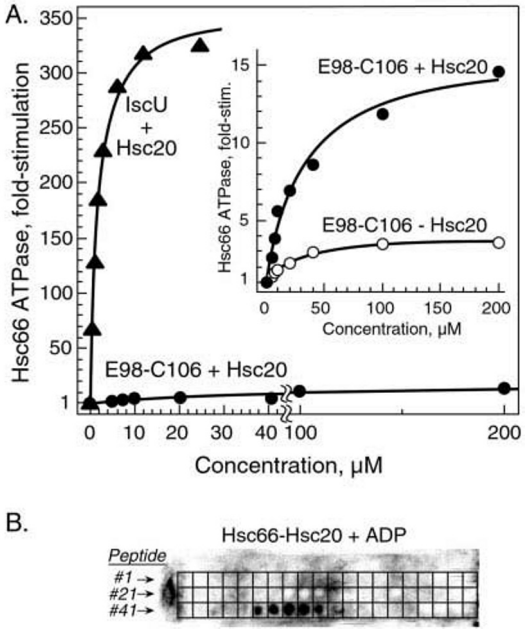

FIG. 5. **Effects of Hsc20 on peptide interactions with Hsc66.** *A*, comparison of IscU and IscU E98-C106 peptide stimulation of Hsc66 ATPase in the presence of 50 μM Hsc20. *Curves* represent best fits to the data with a maximal stimulation of 362-fold and half-maximal stimulation at 1.8 μM for IscU (▲) and 15-fold and 30 μM for the IscU E98-C106 peptide (●). *Inset*, comparison of E98-C106 stimulation in the presence (●) and absence of Hsc20 (○). *B*, 5 μM Hsc66 binding to the IscU peptide array in the presence of 50 μM Hsc20 in HKM buffer containing 1 mM ADP.

were found to occur approximately every 36 residues on average (17). Like Hsc66, DnaK also binds to peptides containing the LPPVK motif consistent with its general preference for peptides with hydrophobic central residues and a basic C terminus. Unlike Hsc66, however, DnaK bound to several other regions of the IscU blot with equal or greater affinity. These results indicate that Hsc66 binding is more specific than that of DnaK, and suggest that Hsc66 does not simply function as a general chaperone with broad substrate specificity.

IscU Peptide Stimulation of Hsc66 ATPase—The specificity of Hsc66 for peptides containing the LPPVK sequence suggests that this segment may be a major determinant for interactions with Hsc66. To investigate whether this region is sufficient to mediate IscU-like interactions with Hsc66, a peptide corresponding to residues 98–106, ELPPVKIHC (E98-C106) of the IscU protein was synthesized. As an initial investigation of the ability of the peptide to interact with Hsc66, we examined its effect on the stimulation of Hsc66 ATPase activity. As shown in Fig. 4, E98-C106 is capable of stimulating the steady-state ATPase activity of Hsc66. Moreover, E98-C106 stimulation of Hsc66 occurs with similar affinity ($K_m \cong 27$ μM) as chaperone stimulation by full-length IscU ($K_m \cong 34$ μM). This binding affinity is within the range of affinities measured for peptide substrates interacting with the ATP state of DnaK (30–32). The correlation between the affinity of Hsc66 for IscU and for the E98-C106 peptide suggests that this is a key region of IscU necessary for binding and the main contributor to the affinity of Hsc66 for IscU. The maximal stimulation of Hsc66 ATPase caused by peptide (4-fold), however, is approximately half that elicited by IscU (7–8-fold). This may reflect the fact that other regions of IscU that do not significantly increase the affinity of Hsc66 for IscU are necessary for maximal stimulation of Hsc66 ATPase activity.

When the peptide SLWPPVSGG (designated PD1) corresponding to the most highly represented phage from affinity panning experiments was examined, it also was found to stimulate the ATPase activity of Hsc66 (Fig. 4). However, the concentration for half-maximal stimulation occurs at a concentration ($K_m > 1$ mM) at least 40-fold higher than that required for the IscU peptide. Because of the low affinity for PD1, it was not possible to determine the maximal stimulation elicited.

Effect of Hsc20 on Hsc66-Peptide Interactions—Hsc20 binds to IscU, and the two proteins synergistically stimulate the ATPase activity of Hsc66 (6). Hydrolysis of ATP converts the chaperone to its high substrate affinity R-state effectively trapping IscU (5). The interactions of Hsc20 with Hsc66 and IscU are typical of the Hsp40-like co-chaperones directing substrate peptides to their chaperone partner (33, 34). To determine whether Hsc20 affects the interaction of Hsc66 with peptides, we examined the peptide-induced stimulation of Hsc66 ATPase activity in the presence of saturating (50 μM) concentrations of Hsc20. In the presence of Hsc20 and E98-C106 there is an increase in the maximal stimulation of Hsc66 ATPase activity to 15-fold (Fig. 5*A*). This is slightly greater than the additive effect of the individual stimulation caused by Hsc20 (~5-fold) and E98-C106 (~4-fold), but is more than 20-fold lower than the synergistic stimulation caused by Hsc20 and full-length IscU (~370-fold). In addition, whereas Hsc20 decreases the concentration of full-length IscU necessary for half-maximal stimulation ($K_m \cong 2$ μM), Hsc20 does not affect the concentration dependence of stimulation by the E98-C106 peptide ($K_m \cong 30$ μM). In similar experiments using PD1, Hsc20 did not affect the affinity of Hsc66 for the PD1 peptide, and the stimulation caused by Hsc20 and PD1 was similar to the additive effect of their individual stimulations (data not shown).

The lack of Hsc20 effects on the affinity of Hsc66 for peptides raised the possibility that Hsc20 might change the region of the IscU protein that is recognized by Hsc66. To investigate this we examined the effect of Hsc20 on the interaction of Hsc66 with the IscU peptide array. Fig. 5*B* shows the binding of Hsc66 to the IscU blot in the presence of 50 μM Hsc20 and 1 mM ADP. Under these conditions, Hsc66 interacts with the same region of IscU (peptides including amino acids 91–111) as in the absence of Hsc20. We also examined the interaction of Hsc20 with the IscU peptide array in the absence of Hsc66 and found that no Hsc20 binding was detected (data not shown). These results indicate that Hsc20 does not change the Hsc66 recognition of IscU. In addition, the inability of Hsc20 to affect the affinity of

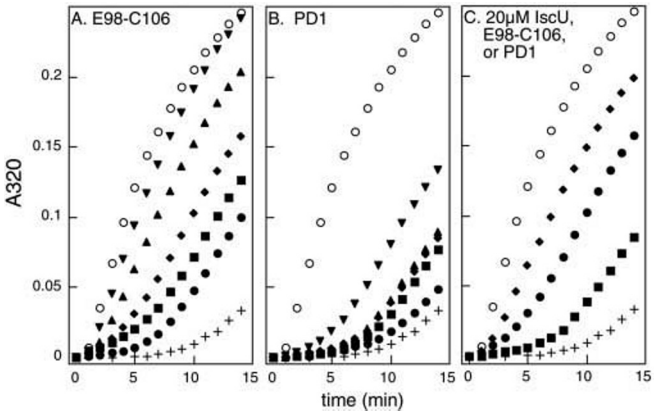

FIG. 6. **Peptide effects on Hsc66 chaperone activity.** Aggregation assays were carried out in HKM buffer containing 1 mM ADP. Denatured rhodanese in 6 M guanidine hydrochloride was diluted into the reaction mixture, and absorbance changes at 320 nm were used to monitor aggregation at 25 °C. *A*, aggregation of 2 μM bovine rhodanese alone (○) or in the presence of 10 μM Hsc66 with 0 (+), 5 (●), 10 (■), 20 (♦), 50 (▲), and 100 μM (▼) E98-C106. *B*, aggregation of 2 μM bovine rhodanese alone (○) or in the presence of 10 μM Hsc66 with 0 (+), 5 (●), 10 (■), 20 (♦), 50 (▲), and 100 μM (▼) PD1. *C*, aggregation of 2 μM bovine rhodanese alone (○), in the presence of 10 μM Hsc66 (+), and Hsc66 with 20 μM IscU (♦), 20 μM E98-C106 (●), or 20 μM PD1 (■).

Hsc66 for IscU peptide and the lack of binding of Hsc20 to the IscU peptide array suggests that Hsc20 does not interact with denatured peptides. The latter finding is in agreement with previous findings in which Hsc20 was unable to prevent the aggregation of the denatured model substrates bovine rhodanese, porcine citrate synthase, and firefly luciferase (3).

Peptides Behave as Hsc66 Substrates—Hsc66 has been shown to prevent the aggregation of the denatured model substrates bovine rhodanese and porcine citrate synthase (3). Because it behaves as a substrate for Hsc66, IscU inhibits the chaperones ability to suppress the aggregation of these model substrates (5). To investigate whether the identified peptides interact with Hsc66·ADP in a manner similar to the IscU protein, we examined their ability to compete with denatured rhodanese for binding to Hsc66. Fig. 6*A* shows the effect of Hsc66·ADP on the aggregation of rhodanese in the presence of varying concentrations of the E98-C106 peptide. Hsc66·ADP suppression of rhodanese aggregation is inhibited by E98-C106 in a concentration-dependent manner. At 15 min a 1:1 molar ratio of peptide to Hsc66 inhibits aggregation suppression by ~45%, and a 10-fold higher molar ratio inhibits the chaperone activity of Hsc66 >95%. E98-C106 alone had no effect on the aggregation of rhodanese (data not shown) suggesting that the changes in turbidity are not because of peptide aggregation or peptide increasing the aggregation of rhodanese.

The effect of the PD1 peptide on Hsc66 chaperone activity was also investigated using the aggregation of bovine rhodanese (Fig. 6*B*). As with E98-C106, the PD1 peptide inhibited the ability of Hsc66·ADP to suppress the aggregation of rhodanese in a concentration-dependent manner. However, PD1 inhibition of Hsc66 chaperone activity occurred to a lower extent than seen for E98-C106, and a 10-fold higher concentration of PD1 was required for 50% inhibition of Hsc66 suppression of rhodanese aggregation. The ability of PD1 to interact with the ADP-bound state of Hsc66 is consistent with the peptide being selected via the affinity panning experiments in which phage were bound to Hsc66 in the presence ADP and eluted by ATP.

We also compared the ability of the peptides to inhibit Hsc66 chaperone activity to that of full-length IscU using a 2:1 ratio of peptide or IscU to Hsc66. Examination of the effect of IscU on the chaperone activity of Hsc66 shows that this molar ratio of IscU to Hsc66 inhibits suppression by ~80% (Fig. 6*C*). This is greater than the inhibition by E98-C106 and PD1, which inhibit Hsc66 ~60 and ~26%, respectively, at this concentration. The increased inhibition caused by IscU may be because of Hsc66·ADP having a greater affinity for the full-length active protein than either of the peptides. Whereas quantitatively different, the general effects caused by the peptides are similar to those of IscU and suggest that the peptides also behave as chaperone substrates.

Hsp70 proteins are composed of two functional domains, an N-terminal ATPase domain and a C-terminal peptide-binding domain (35–37). The C-terminal domain can be further divided into a β-sandwich subdomain that interacts directly with bound peptide and an α-helical lid that lies over the bound substrate (18). We have previously shown that the β-sandwich subdomain, but not the α-helical lid, of Hsc66 is required for IscU binding and stimulation of Hsc66 ATPase (5). To determine whether the selected peptides also interact through this region of Hsc66, we examined their ability to stimulate the ATPase activity of Hsc66 truncation mutants lacking either the α-helical lid (Hsc:2-505) or the entire C-terminal peptide-binding domain (Hsc:2-382) (Fig. 7). As with native IscU, peptides stimulate the activity of both Hsc66 and the Hsc:2-505 mutant lacking the α-helical subdomain. However, neither peptide nor IscU was capable of stimulating the activity of the Hsc:2-382 mutant that lacked the entire peptide-binding domain. Thus, the β-sandwich region of the peptide-binding domain is necessary for peptide interactions with Hsc66, consistent with peptides binding to Hsc66 in a manner similar to the full-length IscU protein.

DISCUSSION

The results described herein provide evidence that Hsc66 substrate specificity differs from other Hsp70 chaperones and that Hsc66 recognizes a specific region of the IscU protein. Phage display affinity panning experiments showed that, as for other Hsp70 substrates (16, 26, 27), Hsc66 substrates are enriched in hydrophobic residues and display an under-representation of acidic amino acids. In contrast to other Hsp70s, however, Hsc66 preferentially selected phage with centrally located proline residues. Furthermore, a large proportion of Hsc66-selected phage contained two adjacent proline residues that were typically located in the center of the displayed heptamer. Taken together, the affinity panning data reveal a consensus sequence of *X*-*X*-Hϕ-Pro-Pro-Hϕ-polar for Hsc66-selected phage.

Experiments investigating the interaction of Hsc66 with cellulose-bound peptides comprising the sequence of IscU reveal that Hsc66 preferentially binds to a single region of the protein. Shared among the bound peptides of the IscU sequence is a pentapeptide sequence, LPPVK, corresponding to residues 99–103. This sequence is similar to the last five positions (Hϕ–Pro–Pro–Hϕ–polar) of the Hsc66 peptide substrate consensus generated from phage display experiments. In contrast, DnaK bound 25 individual peptides corresponding to 5 separate regions of the IscU sequence. The findings with DnaK are consistent with earlier studies that showed that DnaK preferentially binds to regions of denatured proteins that are enriched in hydrophobic residues (16, 17, 29). However, surface probability analysis (46) of the IscU primary sequence reveals that the majority of the peptides recognized by DnaK are likely to be buried in the IscU protein and would therefore be unavailable for DnaK binding. The lack of accessibility of these regions in the native protein may explain why IscU stimulates DnaK ATPase only weakly (5).

The IscU family is one of the most evolutionarily conserved in nature (7, 38), and examination of the amino acids bound by

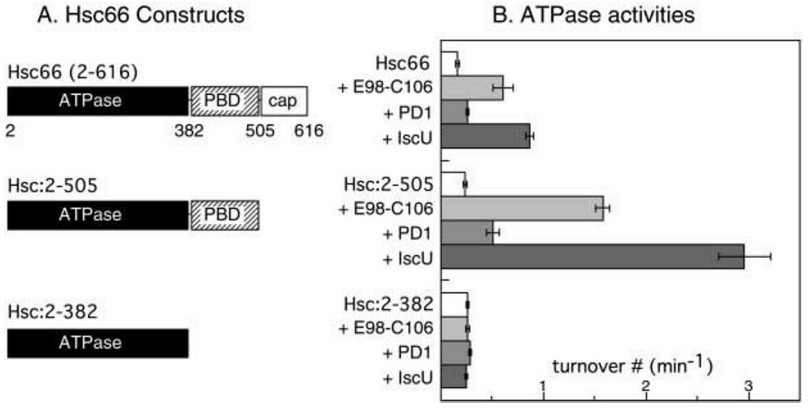

FIG. 7. **Effect of peptides on the ATPase activity of Hsc66 truncation mutants.** *A*, diagrams of the domain composition of Hsc66 constructs. The mature form of full-length Hsc66 contains residues 2–616. *B*, steady-state ATPase activity of 5 μM Hsc66, Hsc:2-505, or Hsc:2-382 alone and in the presence of 100 μM E98-C106, PD1, or full-length IscU in HKM buffer with 1.5 mM ATP at 23 °C. *Error bars* reflect one standard deviation from three independent experiments.

Hsc66 among IscU homologs reveals that the LPPVK motif is invariant among IscU family members identified to date (Fig. 8). The amino acids surrounding this motif also show high sequence similarity suggesting that this evolutionarily conserved region may be an important determinant for IscU family members to interact with their chaperone partner. Our finding that a peptide corresponding to this region is capable of eliciting IscU-like effects on Hsc66 supports this hypothesis. Unlike denatured model protein substrates (3), the E98-C106 peptide is capable of stimulating Hsc66 ATPase activity. This peptide behaves as a substrate for Hsc66, inhibiting the ability of Hsc66 to suppress bovine rhodanese aggregation and requiring the β-sandwich region of the peptide-binding domain for interaction. Thus the LPPVK region appears to be a major determinant for interactions between IscU and Hsc66 and may be the site of interaction for all IscU family members with their chaperone partners. The finding that the E98-C106 peptide binds with affinity similar to that of native IscU suggests that the LPPVK sequence may lie in an unstructured region of the protein. Analysis of the predicted secondary structure of IscU indicates that the LPPVK peptide may occur in a loop between two α-helices and is likely to be surface exposed (39). Examination of the crystal structures of proteins that contain the LPPVK motif, or LPPV or PPVK sequences, reveals that these segments are most commonly found in loop regions frequently near the protein surface.[2] Whereas it seems likely that the LPPVK region will be unstructured, an understanding of its exact position in IscU will require determination of the atomic structure of the protein.

In addition to its interactions with Hsc66, IscU binds to the J-domain co-chaperone Hsc20 and this interaction results in a synergistic stimulation of Hsc66 ATPase activity and an increase in the affinity of Hsc66 for IscU (6). It has been proposed that J-type co-chaperones function as specificity factors for the Hsp70 with which they interact (33, 34, 40, 41), and the interactions of Hsc20 and IscU are consistent with this model (3, 6). Hsc20, however, does not alter the affinity of Hsc66 for the E98-C106 peptide, and the E98-C106 peptide does not synergistically stimulate the chaperone in the presence of Hsc20. These results are similar to those found for DnaJ and σ^{32} stimulation of DnaK ATPase activity in which DnaJ and σ^{32} synergistically stimulate DnaK ATPase activity, whereas DnaJ and σ^{32}-derived peptides do not (34). It has been proposed that the synergism caused by DnaJ and protein substrates allows DnaK to discriminate between peptides and proteins and prevents DnaK from forming unproductive complexes with peptides (34). The synergistic interaction between Hsc20 and IscU may similarly prevent Hsc66 from indiscriminately binding other proteins that display the LPPVK motif and prevent the

```
                    98                  108
E. coli             EELELPPVKIHCSI
N. meningitidis     ----------------
B. aphidicola       ----------------
R. conorii          K--S-----L---L
R. prowazekii       K--S-----L---L
P. multocida        ----------V----
P. aeruginosa       ---A-----------V
C. ruminantium      K--S-----------L
H. influenza        ----------V----
Y. pestis           ----------------
G. lamblia          DK-G-----------V
V. cholera          ----------------
S. pombe            K--C-----L---M
S. cerevisiae 1     K--S-----L---M
S. cerevisiae 2     K--S-----L---M
C. elegans          K--C-----L---M
A. thaliana         KH-S-----L---M
D. melanogaster     K--R-----L---M
M. musculus         K--C-----L---M
H. sapiens 1        K--C-----L---M
H. sapiens 2        K--C-----L---M
```

FIG. 8. **Sequence alignment of the binding site for *E. coli* Hsc66 among IscU homologs.** Alignment of *E. coli* IscU (amino acids 95–108) with IscU family members from prokaryotic and eukaryotic species. Residues identical to *E. coli* IscU are shown as a dash, and the LPPVK motif is *boxed*.

unproductive cycling of Hsc66 ATPase activity. The *E. coli* genome encodes two additional proteins with the LPPVK motif and encodes 33 other proteins that contain LPPV or PPVK sequences, but it is not known whether Hsc66 or Hsc20 interact with these proteins.

The ability of Hsp40 proteins to act as specificity factors may result from their ability to bind substrates at regions separate from their chaperone partner (29, 34, 41), and Hsc20 may recognize a region of IscU distinct from the motif recognized by Hsc66. Hsc20, however, did not bind to individual peptides arrayed on the IscU blot, suggesting that Hsc20, unlike Hsc66, does not interact with an unstructured region of IscU. This finding is consistent with previous studies in which Hsc20 failed to interact with denatured model protein substrates (3) and suggests that IscU must be folded in its native state for interactions with Hsc20. Unlike Hsp40-type co-chaperones, however, Hsc20 lacks the zinc finger and C-terminal regions found to be necessary for binding of denatured substrates (3). In place of these regions Hsc20 has a unique C-terminal domain that the recent x-ray crystal structure revealed to be a three-helix bundle (42). This domain contains a highly con-

[2] Protein Data Bank (www.rcsb.org/pdb/).

served acidic patch that may function to interact with a basic region on the surface of IscU that is not represented by the unstructured peptides.

It is surprising that the peptide identified with the greatest frequency in the affinity panning experiments shows only weak interactions with Hsc66. Whereas the interactions of PD1 with Hsc66 are consistent with its behavior as a chaperone substrate, the lower affinity for ATPase stimulation and the decreased ability to inhibit suppression of rhodanese aggregation indicate that it is not as efficient as the E98-C106 peptide. The high frequency of PD1 among phage bound by Hsc66 may be because of an avidity effect. M13 phage display five copies of the pIII protein on which the heptameric sequences are displayed, and a single phage could be bound by more than one Hsc66 molecule thereby increasing the apparent affinity (43). The results with PD1, however, differ from those obtained using the model substrates rhodanese and citrate synthase. Hsc66 is capable of binding each of these denatured proteins, but neither polypeptide stimulates Hsc66 ATPase activity (3, 5). The effects of PD1 appear to be intermediate between those caused by the exposed hydrophobic patches of denatured model polypeptides that bind but fail to stimulate Hsc66 and those elicited by E98-C106 which stimulates Hsc66 with similar affinity to IscU. This suggests that slight sequence differences in the LPPVK region of IscU may have significant effects on binding affinity and coupling to the stimulation of Hsc66 ATPase. Studies using modified forms of the E98-C106 peptide as well as site-specific mutants of the IscU protein may allow determination of the contributions of individual residues in the LPPVK sequence to IscU-Hsc66 interactions.

The identification of a specific Hsc66 recognition site on IscU raises questions as to the role of the chaperone in the formation of iron-sulfur clusters on the IscU protein. The exact role Hsc66 plays in Fe-S protein biogenesis is not known, but the interaction of Hsc66 with IscU could affect cluster assembly, cluster stability, or the type of cluster formed. These effects could be a consequence of changes in IscU overall structure upon binding to Hsc66 or could be mediated by changes in the immediate region of the Hsc66 interaction site. The LPPVK motif (residues 99–103) is adjacent to Cys^{106}, which may participate in sulfur transfer during Fe-S cluster assembly (44, 45) or may serve as an iron ligand in the cluster (8, 9). In addition, resonance Raman studies have suggested that IscU Fe-S clusters contain at least one non-histidyl nitrogen or non-tyrosyl oxygen ligand (9), and it is possible that Lys^{103} in the LPPVK motif could itself function as a cluster ligand. Binding of Hsc66 to IscU could affect the ability of Cys^{106} or Lys^{103} to participate in Fe-S cluster formation and thereby play a role in determining the rate of cluster formation or cluster stability. *In vitro* studies have shown that IscU can form both [2Fe-2S] and [4Fe-4S] clusters (9), and Hsc66 binding may also play a role in determining which cluster type is favored. Further studies on the ability of IscU to form clusters in the presence of Hsc66 should provide insight to these possibilities.

REFERENCES

1. Seaton, B. L., and Vickery, L. E. (1994) *Proc. Natl. Acad. Sci. U. S. A.* **91,** 2066–2070
2. Vickery, L. E., Silberg, J. J., and Ta, D. T. (1997) *Protein Sci.* **6,** 1047–1056
3. Silberg, J. J., Hoff, K. G., and Vickery, L. E. (1998) *J. Bacteriol.* **180,** 6617–6624
4. Silberg, J. J., and Vickery, L. E. (2000) *J. Biol. Chem.* **275,** 7779–7786
5. Silberg, J. J., Hoff, K. G., Tapley, T. L., and Vickery, L. E. (2001) *J. Biol. Chem.* **276,** 1696–1700
6. Hoff, K. G., Silberg, J. J., and Vickery, L. E. (2000) *Proc. Natl. Acad. Sci. U. S. A.* **97,** 7790–7795
7. Ouzounis, C., Bork, P., and Sander, C. (1994) *Trends Biochem. Sci.* **19,** 199–200
8. Agar, J. N., Zheng, L., Cash, V. C., Dean, D. R., and Johnson, M. K. (2000) *J. Am. Chem. Soc.* **122,** 2136–2137
9. Agar, J. N., Krebs, C., Frazzon, J., Huynh, B. H., Dean, D. R., and Johnson, M. K. (2000) *Biochemistry* **39,** 7856–7862
10. Tokumoto, U., and Takahashi, Y. (2001) *J. Biochem.* (*Tokyo*) **130,** 63–71
11. Strain, J., Lorenz, C. R., Bode, J., Garland, S., Smolen, G. A., Ta, D. T., Vickery, L. E., and Culotta, V. C. (1998) *J. Biol. Chem.* **273,** 31138–31144
12. Garland, S. A., Hoff, K., Vickery, L. E., and Culotta, V. C. (1999) *J. Mol. Biol.* **294,** 897–907
13. Voisine, C., Cheng, Y. C., Ohlson, M., Schilke, B., Hoff, K., Beinert, H., Marszalek, J., and Craig, E. A. (2001) *Proc. Natl. Acad. Sci. U. S. A.* **98,** 1483–1488
14. Lutz, T., Westermann, B., Neupert, W., and Herrmann, J. M. (2001) *J. Mol. Biol.* **307,** 815–825
15. Kim, R., Saxena, S., Gordon, D. M., Pain, D., and Dancis, A. (2001) *J. Biol. Chem.* **276,** 17524–17532
16. Gragerov, A., Zeng, L., Zhao, X., Burkholder, W., and Gottesman, M. E. (1994) *J. Mol. Biol.* **235,** 848–854
17. Rudiger, S., Germeroth, L., Schneider-Mergener, J., and Bukau, B. (1997) *EMBO J.* **16,** 1501–1507
18. Zhu, X., Zhao, X., Burkholder, W. F., Gragerov, A., Ogata, C. M., Gottesman, M. E., and Hendrickson, W. A. (1996) *Science* **272,** 1606–1614
19. Paek, K. H., and Walker, G. C. (1987) *J. Bacteriol.* **169,** 283–290
20. Hesterkamp, T., and Bukau, B. (1998) *EMBO J.* **17,** 4818–4828
21. Atherton, E., and Sheppard, R. C. (1989) *Solid Phase Peptide Synthesis: A Practical Approach*, IRL Press, Oxford, United Kingdom
22. Riddles, P. W., Blakeley, R. L., and Zerner, B. (1979) *Anal. Biochem.* **94,** 75–81
23. Pace, C. N., Vajdos, F., Fee, L., Grimsley, G., and Gray, T. (1995) *Protein Sci.* **4,** 2411–2423
24. Mach, H., Middaugh, C. R., and Lewis, R. V. (1992) *Anal. Biochem.* **200,** 74–80
25. Gill, S. C., and von Hippel, P. H. (1989) *Anal. Biochem.* **182,** 319–326
26. Takenaka, I. M., Leung, S. M., McAndrew, S. J., Brown, J. P., and Hightower, L. E. (1995) *J. Biol. Chem.* **270,** 19839–19844
27. Blond-Elguindi, S., Cwirla, S. E., Dower, W. J., Lipshutz, R. J., Sprang, S. R., Sambrook, J. F., and Gething, M. J. (1993) *Cell* **75,** 717–728
28. Flynn, G. C., Pohl, J., Flocco, M. T., and Rothman, J. E. (1991) *Nature* **353,** 726–730
29. McCarty, J. S., Rudiger, S., Schonfeld, H. J., Schneider-Mergener, J., Nakahigashi, K., Yura, T., and Bukau, B. (1996) *J. Mol. Biol.* **256,** 829–837
30. Pierpaoli, E. V., Gisler, S. M., and Christen, P. (1998) *Biochemistry* **37,** 16741–17648
31. Jordan, R., and McMacken, R. (1995) *J. Biol. Chem.* **270,** 4563–4569
32. Gisler, S. M., Pierpaoli, E. V., and Christen, P. (1998) *J. Mol. Biol.* **279,** 833–840
33. Kelley, W. L. (1998) *Trends Biochem. Sci.* **23,** 222–227
34. Laufen, T., Mayer, M. P., Beisel, C., Klostermeier, D., Mogk, A., Reinstein, J., and Bukau, B. (1999) *Proc. Natl. Acad. Sci. U. S. A.* **96,** 5452–5457
35. Flaherty, K. M., DeLuca-Flaherty, C., and McKay, D. B. (1990) *Nature* **346,** 623–628
36. Chappell, T. G., Konforti, B. B., Schmid, S. L., and Rothman, J. E. (1987) *J. Biol. Chem.* **262,** 746–751
37. Wang, T. F., Chang, J. H., and Wang, C. (1993) *J. Biol. Chem.* **268,** 26049–26051
38. Zheng, L., Cash, V. L., Flint, D. H., and Dean, D. R. (1998) *J. Biol. Chem.* **273,** 13264–13272
39. Chou, P. Y., and Fasman, G. D. (1978) *Annu. Rev. Biochem.* **47,** 251–276
40. Cyr, D. M., Langer, T., and Douglas, M. G. (1994) *Trends Biochem. Sci.* **19,** 176–181
41. Rudiger, S., Schneider-Mergener, J., and Bukau, B. (2001) *EMBO J.* **20,** 1042–1050
42. Cupp-Vickery, J. R., and Vickery, L. E. (2000) *J. Mol. Biol.* **304,** 835–845
43. Levitan, B. (1998) *J. Mol. Biol.* **277,** 893–916
44. Smith, A. D., Agar, J. N., Johnson, K. A., Frazzon, J., Amster, I. J., Dean, D. R., and Johnson, M. K. (2001) *J. Am. Chem. Soc.* **123,** 11103–11104
45. Urbina, H. D., Silberg, J. J., Hoff, K. G., and Vickery, L. E. (2001) *J. Biol. Chem.* **276,** 44521–44526
46. Oxford Molecular Group (1996) *MacVector version 6.0.1*, Oxford Molecular Group PLC, Oxford